

Ultra-compact on-chip LED collimation optics by 3D femtosecond direct laser writing

SIMON THIELE,^{1,*} TIMO GISSIBL,² HARALD GIESSEN,² AND ALOIS M. HERKOMMER¹

¹Institut für Technische Optik and Research Center SCoPE, University of Stuttgart, Stuttgart, Germany

²4th Physics Institute and Research Center SCoPE, University of Stuttgart, Stuttgart, Germany

*Corresponding author: thiele@ito.uni-stuttgart.de

Received 18 April 2016; revised 31 May 2016; accepted 1 June 2016; posted 1 June 2016 (Doc. ID 263376); published 27 June 2016

By using two-photon lithographic 3D printing, we demonstrate additive manufacturing of a dielectric concentrator directly on a LED chip. With a size of below 200 μm in diameter and length, light output is increased by a factor of 6.2 in collimation direction, while the emission half-angle is reduced by 50%. We measure excellent form fidelity and irradiance patterns close to simulation. Additionally, a more complex shape design is presented, which exhibits a nonconventional triangular illumination pattern. The introduced method features exceptional design freedoms which can be used to tailor high-quality miniature illumination optics for specific lighting tasks, for example, endoscopy. © 2016 Optical Society of America

OCIS codes: (220.2945) Illumination design; (220.4000) Microstructure fabrication; (220.3740) Lithography; (230.3670) Light-emitting diodes.

<http://dx.doi.org/10.1364/OL.41.003029>

Additive manufacturing of optical components in three dimensions is a fast-growing research field [1–8]. Different approaches, such as inkjet printing or stereolithography are used, and corresponding printers are commercially available. With resolutions of <100 nm and optically clear materials, direct laser writing by two-photon lithography is ideally suited for the fabrication of optical elements in the micrometer regime [2]. A variety of different micro- and nano-optical components, created by femtosecond direct laser writing, have been successfully demonstrated in recent years. These include photonic crystals [3], optical waveguides [4], diffractive elements [5], and refractive freeform surfaces [6], as well as hybrid diffractive-refractive elements [7], and even multi-component optical systems [8,9].

Due to the simple processing requirements, femtosecond direct laser writing is compatible with a variety of substrates. The chemical structure of the resists enables strong adhesion on many different surfaces. Optical elements have been manufactured directly on optical fibers [10] or integrated photonic circuit chips [4]. The direct fabrication on optoelectronic surfaces such as emitting areas of light emitting diodes (LED) or vertical cavity lasers (VCSELs), as well as on the pixel matrix of image sensors, is easily feasible.

LED chips today are crucial components for many optical applications and can be miniaturized down to the micrometer scale. However, influencing the light output distribution on the same scale has proved challenging. Integrated photonic structures can change the radiation characteristics of bare LED chips and decrease their étendue [11]. Similarly, chip-integrated reflective sidewalls are used to decrease the angular extent of the source [12], although only by small amounts. Refractive primary optics that transform the mostly Lambertian emission patterns usually consist of simple domes with diameters considerably greater than the active area of the chip. Schreiber *et al.* reported on diamond turned concentrators as primary optics [13], although with dimensions roughly a factor of ten above the optics presented here. An example of collimation optics by femtosecond direct laser writing was published by Jiang *et al.* [14]. However, in this case, a laser diode with high spatial coherence was used. This requires a different design approach for collimation compared to our LED case and does not require an undercut design, as is presented here.

Efficient primary optics play a crucial role for the miniaturization of LED illumination systems. In principle, two types of primary optics can be distinguished. In the first case, the lens is placed with an air gap above the chip. This helps in étendue-critical applications because étendue is not raised due to a higher index material being in contact with the chip [15]. In the second case, a material with a refractive index higher than air is in contact with the LED chip.

This increases the overall efficiency because less total internal reflection (TIR) happens at the boundary between the chip with its high refractive index and the outside world.

A miniaturized primary optics can significantly reduce the size and shape requirements for the secondary optics and, thus, help to decrease the total system dimensions. In this Letter, we demonstrate the usefulness of additive manufacturing to create a new class of on-chip LED optics with unprecedented design freedom and unmatched optical properties on this length scale. In the following, the design, fabrication, and experimental characterization are described.

The ray tracing design starts with modeling of the LED source. For the experiments, an InGaAs point source chip (OSRAM F1372B) with a circular emitting area of $80 \mu\text{m}$ in diameter was used. The center wavelength is 650 nm, and the emission pattern is Lambertian. The star-shaped Au

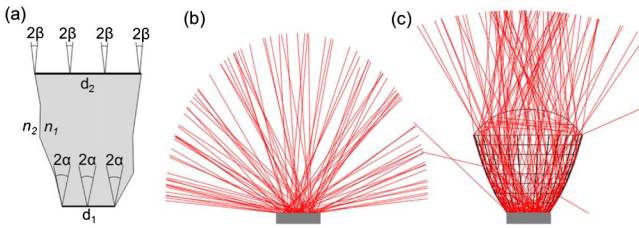


Fig. 1. (a) Illustration of Eq. (1). (b) Cross-sectional view of random source rays, emitted from the bare chip. (c) Effects of the designed compound parabolic concentrator collimator.

electrodes [Fig. 2(a)] are considered in the model with a reflectivity of 100%. With our fabrication approach, the diameter of the optical element cannot exceed 200 μm , which limits the achievable collimation. In the case of conservation of energy, the light output angle is given by

$$\beta = \sin^{-1} \left(\frac{n_1 d_1 \sin(\alpha)}{n_2 d_2} \right), \quad (1)$$

in dependence of the inside and outside refractive indices n_1 and n_2 , input diameter d_1 , output diameter d_2 , and the input angle α (Fig. 1). In this Letter, the refractive index n_1 of the used photoresist was measured to be 1.5101 at 650 nm. Considering a half-angle of 60° at FWHM radiant intensity for the Lambertian emitter, the best achievable half-angle of the current setup in air is thus 31.4° , if étendue is conserved.

Because of the broad angular spectrum of the LED chip, a dielectric total internal reflecting concentrator (DTIRC) [16] was chosen as a first stage of collimation. An aspheric lens

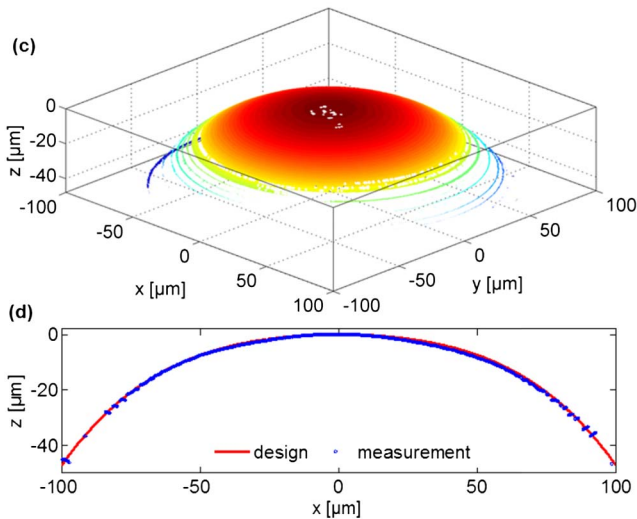
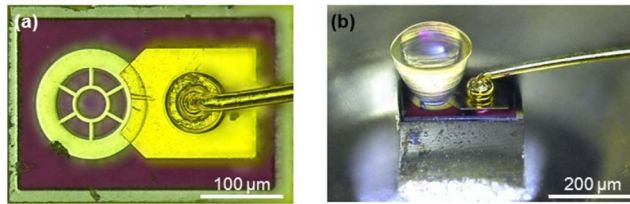


Fig. 2. Fabrication results. (a) LED chip before processing. (b) LED after processing. (c), (d) Chromatic-confocal surface measurement of the top lens surface.

on top provides additional degrees of freedom to influence the final light output. While the DTIRC was designed from analytical considerations, the aspheric top surface was iteratively optimized to achieve a maximum optical power at a predefined target area and to correct for effects of the electrode pattern. The shape of the DTIRC part is defined according to [17] through the coordinate r in radial direction as a function of coordinate z along the symmetry axis [Eq. (2)]:

$$r = \frac{-b + \sqrt{b^2 - 4ac}}{2a}, \quad \text{where}$$

$$a = C^2,$$

$$b = 2(CSz + r_0 P^2),$$

$$c = z^2 S^2 - 2r_0 CQz - r_0^2 PT,$$

$$C = \cos(\theta), S = \sin(\theta), P = 1 + S,$$

$$Q = 1 + P, \quad \text{and} \quad T = 1 + Q. \quad (2)$$

The two parameters, emission radial aperture r_1 and maximum top angle β , are set to 39 μm and 15° , respectively.

The top aspheric surface is defined as a function of radius r as

$$z = \frac{cr^2}{1 + \sqrt{1 - c^2 r^2}} + a_2 r^2 + a_4 r^4 + a_6 r^6, \quad (3)$$

with a curvature c of $-2.858 \cdot 10^{-3} \mu\text{m}^{-1}$ and the aspheric coefficients $a_2 = -9.88 \cdot 10^{-4} \mu\text{m}^{-1}$, $a_4 = -2.26 \cdot 10^{-7} \mu\text{m}^{-3}$, and $a_6 = -1.46 \cdot 10^{-13} \mu\text{m}^{-5}$. Figure 1 depicts ray tracing plots for the source, as well as for the combined system.

To facilitate testing, the LED chips are processed on TO-18 metal packages. The femtosecond direct laser writing is carried out using the commercially available lithography system Photonic Professional GT from the company Nanoscribe GmbH. The photoresist IP-S, specifically developed for smooth surfaces, is used [18].

Details about the dip-in lithography process can be found in [9]. Figure 2 shows the chip before and after processing. In Fig. 3 the final structure is compared to a standard LED in a traditional package with a base diameter of 5 mm.

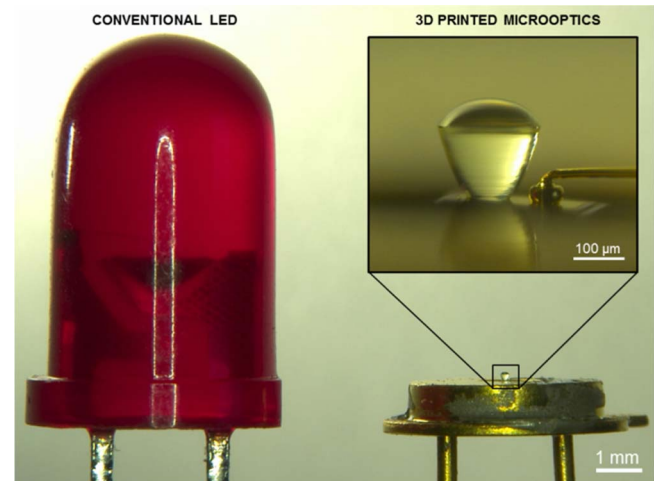


Fig. 3. Size comparison of the 3D printed compound parabolic concentrator lens on top of a chip in a TO-18 package with a conventional 5 mm LED in traditional package.

As visible in the microscope images, the resulting structure exhibits a smooth surface appearance similar to glass. The shape fidelity after fabrication is characterized by measurement of the top aspheric surface with a chromatic-confocal sensor. Comparison between design and measurement exhibits good agreement. AFM measurements from previous work reveal a RMS roughness of ~ 13 nm on comparable lenses, fabricated with the same method and similar parameters. On steeper flanks, the staircase effect of the layer-by-layer writing is still visible, an effect which can be reduced by smaller layer spacing or a contour-based writing algorithm.

In this case, the layer spacing is set to 100 nm as trade-off between writing time and accuracy. The total time to write the structure is about 3.5 h. There are a number of possibilities to increase the writing speed. For example, the process time can be reduced by writing a shell only and flood exposing the sample afterward [7].

Before and after fabrication, the LEDs are tested with a forward current of 10 mA, and the irradiance distribution is recorded. For the measurement, the LED is placed below a

diffuser plate with Lambertian scattering properties [Fig. 4(a)]. The distance between LED and diffuser is chosen far enough to ensure that the emission area of the optics (diameter: 200 μm) can be considered as point source.

The light distribution on the diffuser is imaged with a standard DSLR camera, while the lateral scale is determined by imaging a ruler.

The raw data images are recorded and converted to a data array after linear pixel readout and merging the four RGGB pixels. For comparison with simulation, the irradiance distribution on a detector at the same distance as in the experiment is calculated by ray tracing. Effects such as multiple Fresnel reflections and reflections at the Au electrodes are taken into account.

The results of simulation and experiment are shown in Figs. 4(b)–4(e). If light output is compared in forward direction, the DTIRC structure shows an increase in irradiance by a factor of 6.2 compared to the bare chip. This value is considerably higher than initially proposed by simulation (3.01). The reason for this difference lies in the fact that a higher index material on the emission area of the chip leads to an overall increase in light extraction efficiency compared to air.

The increase can be calculated according to Eq. (4), which considers the change in critical TIR angle inside the chip in dependence of the two refractive indices n_{LED} and n_{Resist} [19]:

$$\frac{\eta_{\text{IP-S}}}{\eta_{\text{air}}} = \frac{1 - \cos\left(\text{asin}\left(\frac{n_{\text{Resist}}}{n_{\text{LED}}}\right)\right)}{1 - \cos\left(\text{asin}\left(\frac{1}{n_{\text{LED}}}\right)\right)}. \quad (4)$$

While the refractive index of the polymerized photoresist $n_{\text{IP-S}}$ is known to be 1.5101, it was not possible to determine the refractive index of the LED top layer due to confidentiality. It is reasonable however, to assume GaAs as material [20], which has a refractive index of 3.83 at $\lambda = 650$ nm. This would lead to an increase in extracted power by a factor of 2.33. Combined with the increase by collimation, a factor of 6.6 results, which is not far from the measured value of 6.2. The remaining difference can be explained by scattering losses at writing layers and other imperfections of the structure.

In general, simulation and experiment match well. For better comparison, polar plots of radiant intensity as a function of angle are displayed in Fig. 4(e). The values were calculated by multiplying the irradiance with the squared Cartesian distance between source and point of interest and dividing the results by the cosine of the polar angle [21]. While the simulation and the experiment show similar Lambertian distributions in the case of the bare chip, the curves differ more visibly in the case of the collimation optics. This effect can be explained by deviations from design in the DTIRC shape. The measured FWHM half-angles [Fig. 4(e)] of radiant intensity are very close to the theoretical limit of 31.4° in the case of conservation of energy. The observation that the value seems to be slightly below this limit indicates that the designed efficiency is not fully reached.

The high degree of design freedom of the presented manufacturing method allows for more complex designs, especially when compared to competing technologies such as high precision micromachining or top-down wafer level manufacturing. The arbitrary and efficient redistribution of light is limited in the case of a high spatial and angular extent of the source in comparison with the optics. Nonetheless, it is possible to create unconventional irradiance patterns as well. As an example, a design consisting of three split branches is created, leading

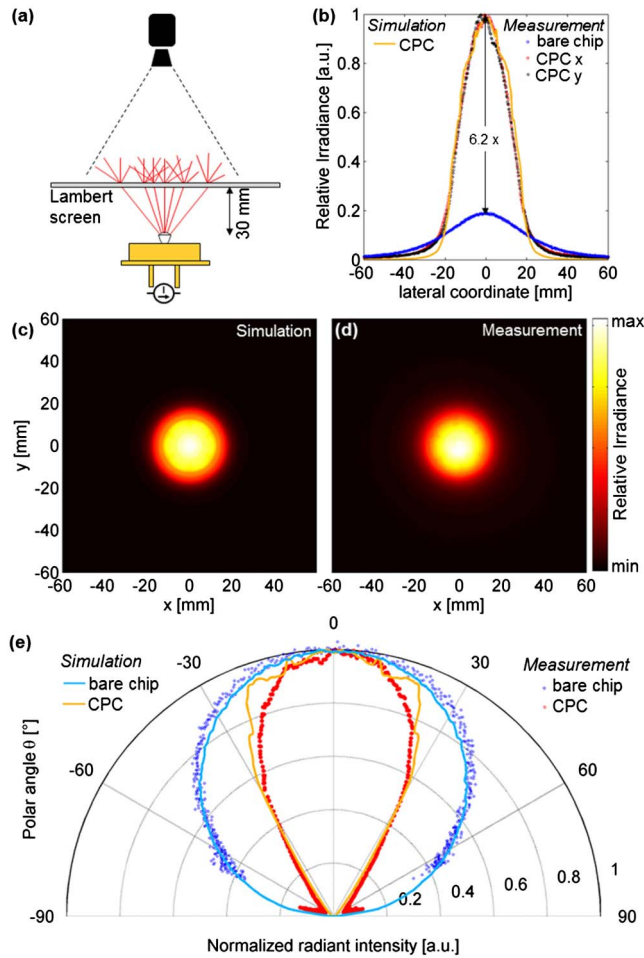


Fig. 4. Characterization. (a) Test setup using a Lambertian screen. (b) Cross section of measured and simulated irradiance. The measured curve of the bare chip is scaled together with the corresponding curve of the DTIRC which is normalized to its maximum. (c), (d) Comparison of measured and simulated irradiance distributions, normalized to their maximum, respectively. (e) Normalized radiant intensity in polar representation.

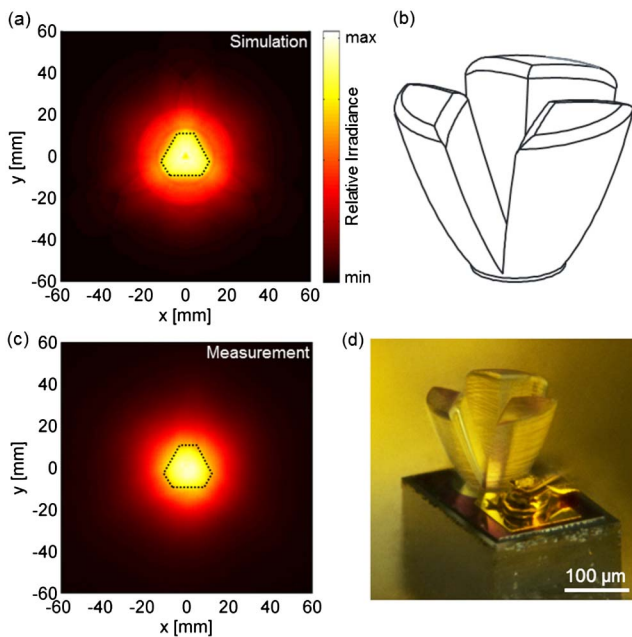


Fig. 5. (a) Simulated irradiance distribution of a nonconventional collimator optics. (b) CAD representation. (c) Measured irradiance distribution. (d) Microscope image of the structure. The black dotted lines in (a) and (c) are equal in size and are guides to the eye for better comparison.

to an irradiance distribution with a triangular shape. Figure 5 shows the comparison of simulated and measured irradiance patterns, as well as the results of the 3D printing. The simulation and experiment show a good matching; the designed shape is well reproduced by the 3D printing.

In conclusion, we have successfully demonstrated a highly miniaturized primary optics, directly manufactured on a LED chip by femtosecond direct laser writing. To the best of our knowledge, the presented device provides unprecedented collimation efficiency in terms of its size. The achieved results match well with theoretical considerations and exhibit high collimation efficiency and high quality of the optics. The method enables an arbitrary geometric complexity at a very small scale and, thus, is perfectly suited for miniaturized devices. While the high writing times prevent a cost-effective mass manufacturing at the moment, small volume production becomes more attractive due to the low initial cost. For the future, multiple approaches such as shell writing or parallelization (using multiple beams through holographic beam splitters [22]) promise to help reducing the writing time drastically. We expect this method to be important for a number of applications such as endoscopic lighting, proximity sensing, and communication or signaling. Special use is assumed for rapid prototyping due to the cheap and short design to manufacturing transfer.

Acknowledgment. The authors thank Dr. Wolfgang Huber from “Chips 4 Light GmbH” for the generous supply of LED chips. Special thanks go to Marion Hagel from Max Planck Institute for Solid State Research for rebonding the chips. The authors also acknowledge support from BW Stiftung (Spitzenforschung II), ERC (Complexplas), DFG, BMBF (PRINTOPTICS), and Carl Zeiss Stiftung.

REFERENCES

1. R. Blomaard and J. Biskop, *NIP & Digital Fabrication Conference* (2015).
2. A. Žukauskas, G. Batavičiūtė, M. Ščiuka, T. Jukna, A. Melninkaitis, and M. Malinauskas, *Opt. Mater. Express* **4**, 1601 (2014).
3. M. Deubel, G. V. Freymann, M. Wegener, S. Pereira, K. Busch, and C. M. Soukoulis, *Nat. Mater.* **3**, 444 (2004).
4. N. Lindenmann, G. Balthasar, D. Hillerkuss, R. Schmogrow, M. Jordan, J. Leuthold, W. Freude, and C. Koos, *Opt. Express* **20**, 17667 (2012).
5. Y. Li, Y. Yu, L. Guo, C. Chen, L. Niu, A. Li, and H. Yang, *J. Opt.* **12**, 035203 (2010).
6. T. Gissibl, S. Thiele, A. Herkommer, and H. Giessen, “Sub-micrometre accurate free-form optics by three-dimensional printing on single-mode fibres,” *Nat. Commun.* (2016), doi: 10.1038/ncomms11763.
7. M. Malinauskas, A. Zukauskas, V. Purlys, K. Belazaras, A. Momot, D. Paipulas, R. Gadonas, A. Piskarskas, H. Gilbergs, A. Gaidukeviciute, I. Sakellari, M. Farsari, and S. Juodkazis, *J. Opt.* **12**, 124010 (2010).
8. A. Žukauskas, M. Malinauskas, and E. Brasselet, *Appl. Phys. Lett.* **103**, 181122 (2013).
9. T. Gissibl, S. Thiele, A. Herkommer, and H. Giessen, “Two-photon direct laser writing of ultracompact multi-lens objectives,” *Nat. Photonics* (2016), doi: 10.1038/nphoton.2016.121.
10. S. Bianchi, V. P. Rajamanickam, L. Ferrara, E. Di Fabrizio, C. Liberale, and R. Di Leonardo, *Opt. Lett.* **38**, 4935 (2013).
11. J. J. Wierer, M. R. Krames, J. E. Epler, N. F. Gardner, M. G. Craford, J. R. Wendt, J. A. Simmons, and M. M. Sigalas, *Appl. Phys. Lett.* **84**, 3885 (2004).
12. M. Ma, J. Cho, E. F. Schubert, Y. Park, G. B. Kim, and C. Sone, *Appl. Phys. Lett.* **101**, 141105 (2012).
13. P. Schreiber, S. Kudaev, R. Steinkopf, and H. Schmidt, “Concentrators for high-power LEDs,” *Fraunhofer Annual Report* (2004), p. 29.
14. T. Jiang, Q. D. Chen, J. Zhang, Z. N. Tian, L. G. Niu, Q. S. Li, H. Y. Wang, L. Qin, and H. B. Sun, *Opt. Lett.* **38**, 3739 (2013).
15. W. Mönch, *Adv. Opt. Technol.* **4**, 79 (2015).
16. J. Chaves, *Introduction to Nonimaging Optics* (CRC Press, 2008).
17. W. T. Winston and R. Welford, *The Optics of Non-imaging Concentrators* (Academic, 1978).
18. <http://www.nanoscribe.de/en/products/ip-photoresists/>.
19. M. Ma, F. W. Mont, X. Yan, J. Cho, E. F. Schubert, G. B. Kim, and C. Sone, *Opt. Express* **19**, A1135 (2011).
20. R. Wirth, C. Karnutsch, S. Kugler, and K. Streubel, *IEEE Photon. Technol. Lett.* **13**, 421 (2001).
21. R. J. Koschel, *Illumination Engineering* (Wiley, 2013).
22. L. Yang, A. El-Tamer, U. Hinze, J. Li, Y. Hu, W. Huang, J. Chu, and B. Chichkov, *Opt. Laser Eng.* **70**, 26 (2015).